Syndecan-4 Knockout Leads to Reduced Extracellular Transglutaminase-2 and Protects against Tubulointerstitial Fibrosis

Alessandra Scarpellini,* Linghong Huang,[†] Izhar Burhan,* Nina Schroeder,* Muriel Funck,* Timothy S. Johnson,[†] and Elisabetta A.M. Verderio[†]

*School of Science and Technology, Biomedical, Life and Health Research Centre, Nottingham Trent University, Nottingham, United Kingdom; and [†]Academic Nephrology Unit, Sheffield Kidney Institute, University of Sheffield, Sheffield, United Kingdom

ABSTRACT

Transglutaminase type 2 (TG2) is an extracellular matrix crosslinking enzyme with a pivotal role in kidney fibrosis. The interaction of TG2 with the heparan sulfate proteoglycan syndecan-4 (Sdc4) regulates the cell surface trafficking, localization, and activity of TG2 *in vitro* but remains unstudied *in vivo*. We tested the hypothesis that Sdc4 is required for cell surface targeting of TG2 and the development of kidney fibrosis in CKD. Wild-type and Sdc4-null mice were subjected to unilateral ureteric obstruction and aristolochic acid nephropathy (AAN) as experimental models of kidney fibrosis. Analysis of renal scarring by Masson tri-chrome staining, kidney hydroxyproline levels, and collagen immunofluorescence demonstrated progres-sive fibrosis associated with increases in extracellular TG2 and TG activity in the tubulointerstitium in both models. Knockout of Sdc-4 reduced these effects and prevented AAN-induced increases in total and active TGF-β1. In wild-type mice subjected to AAN, extracellular TG2 colocalized with Sdc4 in the tubular interstitium and basement membrane, where TG2 also colocalized with heparan sulfate chains. Hepariti-nase I, which selectively cleaves heparan sulfate, completely abolished extracellular TG2 in normal and diseased kidney sections. In conclusion, the lack of Sdc4 heparan sulfate chains in the kidneys of Sdc4-null mice abrogates injury-induced externalization of TG2, thereby preventing profibrotic crosslinking of ex-tracellular matrix and recruitment of large latent TGF-β1. This finding suggests that targeting the TG2-Sdc4 interaction may provide a specific interventional strategy for the treatment of CKD.

CKD is characterized by glomerulosclerosis and tubulointerstitial fibrosis that result from excessive extracellular matrix (ECM) accumulation.[1–3] In re-cent years, the role of transglutaminase type 2 (TG2) has been shown to be crucial to both the ECM expansion[1,4,5] and TGF-β1 activation[6–9] that underlies this fibrotic remodeling.

TG2 belongs to the eight-member transgluta-minase family that catalyzes a calcium-dependent acyl-transfer reaction (EC 2.3.2.13) between the γ-carboxamide group of peptide-bound glutamine and the ε-amino group of peptide-bound lysine,[10] generating stable ε-(γ-glutamyl)-lysine isopeptide crosslinks. In fibrotic diseases (*e.g.*, renal, liver, and pulmonary fibrosis), increased TG2 externalization and/or expression results in abundant crosslink formation, contributing to ECM accumula-tion.[5,7,11–16] In early CKD, ε-(γ-glutamyl)-lysine
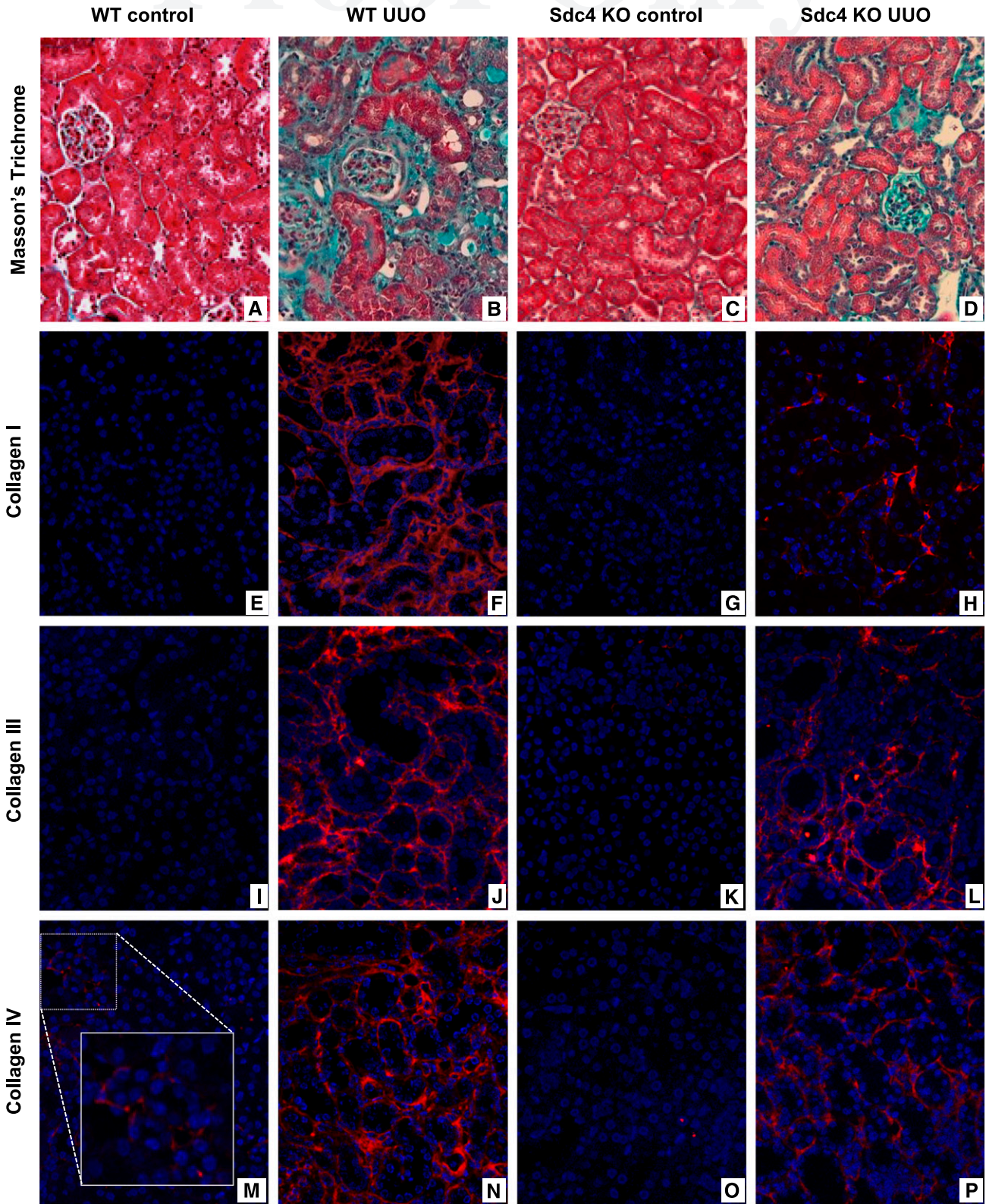
Figure 1. Protective effect of Sdc44-KO on the development of renal fibrosis in the UUO model of CKD. Paraffin sections from WT and Sdc4 KO kidneys (control and 21 days after UUO) were stained with MT (A–D), collagen I (E–H), collagen III (I–J), and collagen IV (M–P). Collagen staining (red) and nuclei staining (blue). Representative images at ×200 magnification are shown. Detail of collagen IV staining at ×400 magnification is shown (M).

crosslinking in the ECM results predominantly from cell externalization of existing TG2 as the renal TG2 level remains constant.[4] The externalized TG2 is known to exert a profibrotic function also through a nonenzymatic "structural" activity, by enhancing arginine-glycine-aspartic acid–independent cell adhesion and, consequently, contraction of the
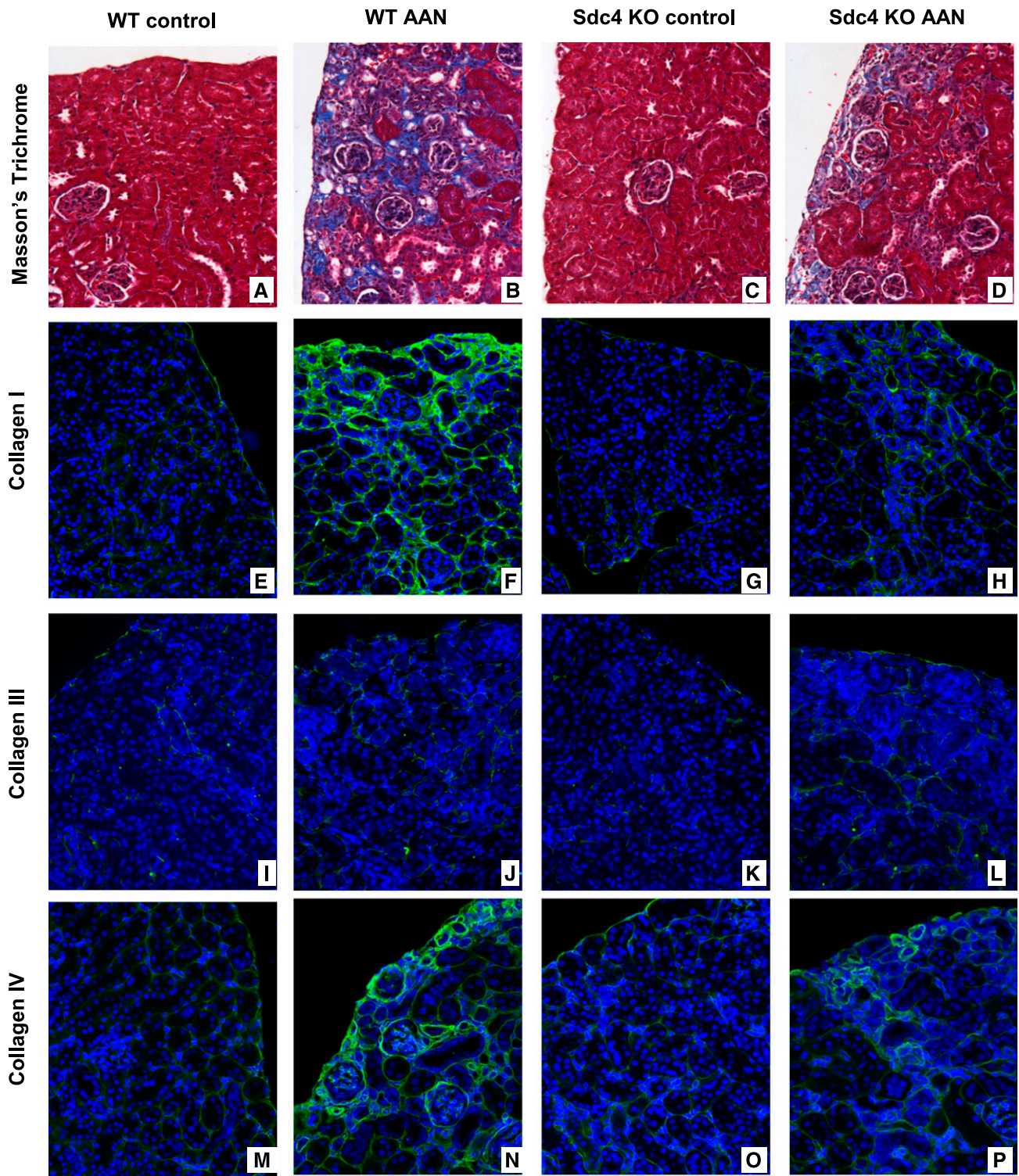

Figure 2. Protective effect of Sdc4-KO of the development of renal fibrosis in the AAN model of CKD. Paraffin sections from WT and Sdc4 KO kidneys (control and AAN at 12 weeks) were stained with MT (A–D), collagen I (E–H), collagen III (I–L), and collagen IV (M–P). Collagens staining (green) and nuclei staining (blue). Representative images at ×200 magnification are shown.

ECM.[17–19] In experimental CKD, pan TG inhibition preserved kidney function because of a reduction in kidney fibrosis in both diabetic and nondiabetic disease.[2,16] Mice deficient in TG2 were protected against the development of fibrosis in obstructive nephropathy resulting from impaired collagen I synthesis related to decreased TGF-β1 activation.[8]

However, clinical application of anti-TG2 therapy has been prevented by the inability to develop TG2-specific inhibitors due to a highly conserved catalytic core across the TG family,[10] with inhibition of factor XIIIa and the keratinocyte transglutaminase causing particular concern.[20] Consequently, elucidation of the mechanism whereby TG2 is released from cells has been an object of intense scrutiny, because TG2 is unconventionally secreted via a potentially unique non-Golgi route,[21,22] which may offer a specific interventional strategy to decrease extracellular TG2.

Recently, we have shown that heparan sulfate proteoglycans (HSPG), such as syndecan-4 (Sdc4), may have a key role in the cell surface trafficking of TG2 in vitro.[23] Sdc4 and TG2 coassociated in cell membranes via the HS chains of Sdc4, for which TG2 has high affinity.[18,23,24] Lack of Sdc4/HS or functional inhibition of HS led to a lower level of cell-surface TG2 antigen and crosslinking activity in vitro and a parallel accumulation of cytosolic TG2 with no changes in the total level of TG2 expression.[23] Membrane-proximal Sdc4/HS may, therefore, affect the unconventional secretion of TG2, as described for fibroblast growth factor-2, by acting as a cell-surface "molecular trap."[25] Therefore, Sdc4/HS may modulate TG2 profibrotic function by controlling its cell-surface trafficking. Sdc4/HS has also been implicated in kidney fibrosis, being upregulated in progressive proliferative kidney diseases (IgA nephropathy) and diabetic nephropathy, but not in nonproliferative diseases.[26–28]

To investigate the possible role of Sdc4 in regulating cell-surface trafficking of TG2 in vivo, we induced kidney fibrosis in Sdc4-knockout (KO) mice[29] and assessed whether or not Sdc4 deletion affected TG2 externalization/extracellular activity and tubulointerstitial fibrosis development. We used two distinct experimental models of kidney fibrosis: unilateral ureteric obstruction (UUO)[30] and aristolochic acid nephropathy (AAN).[31,32] Sdc4-KO ameliorated tubulointerstitial fibrosis in both models, and deletion of Sdc4 led to a lowering of extracellular TG2 in the ECM. Binding of TG2 to the tubular interstitium depended on the HS chains of proteoglycans, with which TG2 was found to be strongly associated in normal and diseased kidney. These data suggest for the first time that Sdc4
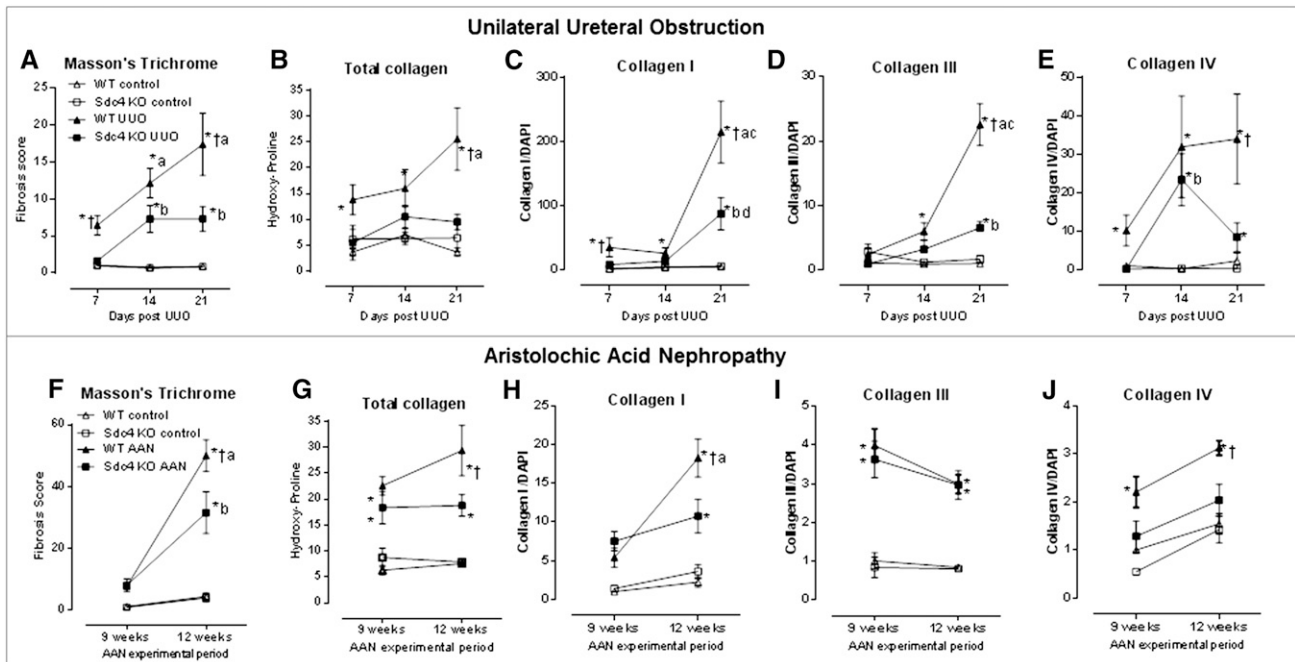

Figure 3. Quantification of the protective effect of Sdc4 in the UUO and AAN models of CKD. Graphical presentation of kidney fibrosis in the UUO (A–D) and AAN (E–H) fibrotic lesions. The fibrosis score was calculated by multiphase analysis of MT-stained kidney sections as the ratio blue/green (collagen)/pink/red (tissue area) (A and E). Deposition of collagen I (B and F), collagen III (C and G), and collagen IV (D and H) was measured by multiphase analysis of immunofluorescence-stained kidney sections (collagens/DAPI). All data were normalized by the WT control at the lower time point (day 7 for UUO, week 9 for AAN). Raw data at these time points were the following: MT UUO, 0.02; MT AAN, 0.001; collagen I UUO, 0.01; collagen I AAN, 0.03; collagen III UUO, 0.04; collagen III AAN, 0.06; collagen IV UUO, 0.03; collagen IV AAN, 0.08. *$P<0.05$ versus control; $^{\dagger}P<0.05$ versus Sdc4-KO UUO or AAN; $^{a}P<0.05$ versus WT day 7 UUO or week 9 AAN; $^{b}P<0.05$ versus Sdc4-KO day 7 UUO or week 9 AAN; $^{c}P<0.05$ versus WT day 14 UUO; $^{d}P<0.05$ versus Sdc-KO day 14 UUO.

plays a critical role in the pathogenesis of kidney fibrosis by regulating TG2 trafficking and localization *via* HS chain-binding.

RESULTS

Kidney Fibrosis Is Reduced in Sdc4-Null Mice

The phenotype of Sdc4-KO mice was investigated in two models of CKD: UUO and AAN. Both models led to the progressive development of interstitial fibrosis in wild-type (WT) kidneys as assessed by Masson trichrome (MT) staining (Figures 1, A and B, and 2, A and B). Fibrotic areas caused by Aristolochic acid I (AAI) were mainly located in the outer cortex with areas of scarred tissue tracking down the medullary ray, whereas in the UUO, there was a more diffuse fibrosis through the cortex. Sdc4 deletion resulted into a reduced collagen staining in both models compared with WT (Figures 1D and 2D). There were no differences between WT and Sdc4-KO kidneys at baseline (Figures 1, A and C, and 2, A and C).

Multiphase image analysis of collagen-positive staining on MT sections revealed that in the UUO model the increase in collagen was significant compared with the change in controls at all the time points ($P<0.05$) (Figure 3A), while differences between WT and Sdc4-KO fibrotic kidneys were significant at days 7 and 21 after UUO (Figure 3A). In the AAN model, MT staining was significantly higher than the control at 12 weeks (Figure 3F), with a reduction of MT staining in the Sdc4-KO compared with WT fibrotic kidneys (Figure 3F). In both models, fibrosis development was slower in Sdc4-KO mice than in the WT (Figure 3, A and F). Whole-kidney hydroxyproline analysis confirmed the progressive increase of collagen in both models of fibrosis, with lower collagen accumulation in Sdc4-KO at day 21 after UUO and at 12 weeks in the AAN model (Figure 3, B and G).

Individual changes in the levels of collagen I, III, and IV were analyzed by immunofluorescence on paraffin sections from WT and Sdc4-KO kidneys. There were no significant differences in any collagen staining in control kidneys between WT and Sdc4-KO mice (Figures 1 and 2, E, G, I, K, M, O). All collagens were increased in diseased kidneys, particularly so in WT kidneys (Figures 1 and 2, F, J, N) compared with Sdc4-KO kidneys (Figures 1 and 2,

H, L, P). These differences were confirmed by multiphase image analysis of the staining for collagen I (Figure 3, C and H), collagen III (Figure 3, D and I), and collagen IV (Figure 3, E and J) from both CKD models. In diseased animal, kidneys from Sdc4-KO mice showed reduced levels of collagen I deposition compared with WT at days 7 and 21 in the UUO model (Figure 3C) and at 12 weeks in the AAN model (Figure 3H). Lower levels of collagen III accumulation were also detected at day 21 in Sdc4-KO obstructed kidneys (UUO) compared with WT (Figure 3D), but not in response to AAI (Figure 3I). Changes in collagen IV, typically abundant in the tubular and glomerular basement membranes, were greater in the WT than in the Sdc4-KO obstructed kidneys at 21 days after UUO (Figure 3E) and at 12 weeks in the AAN model (Figure 3J). Evaluation of collagen gene expression by qualitative RT-PCR analysis revealed significant elevation of interstitial collagen $\alpha1(I)$ and collagen III transcripts and the
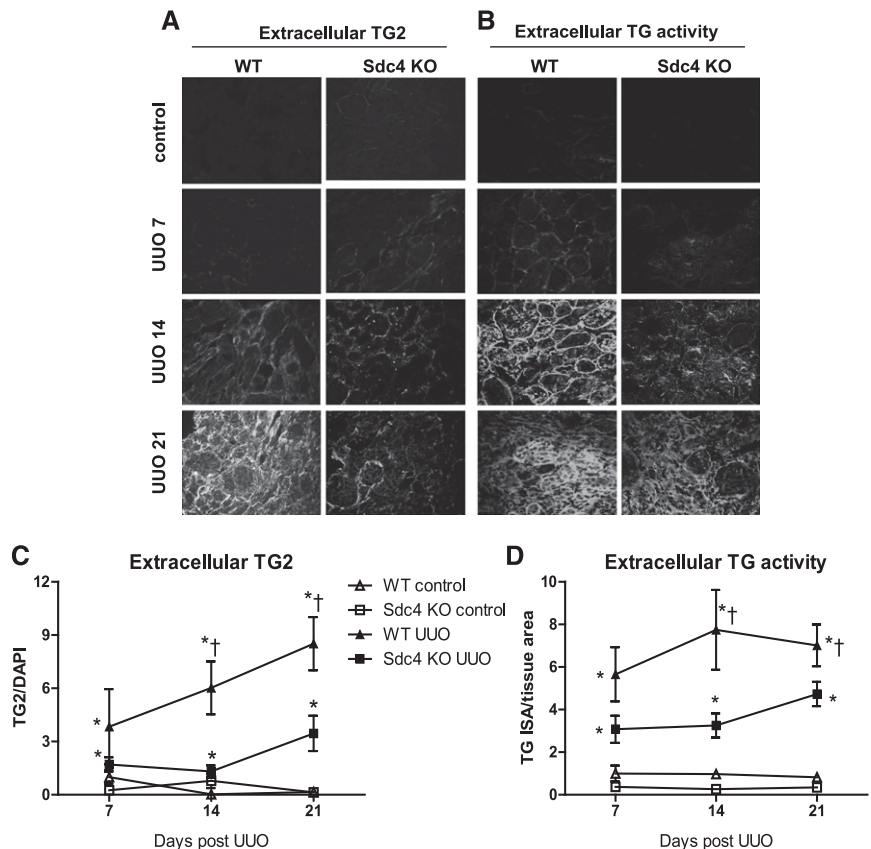

Figure 4. Sdc4-KO decreases extracellular TG2 and TG activity in the UUO model of CKD. Extracellular TG2 and TG *in situ* activity (ISA) were detected on cryostat sections of WT and Sdc4 KO kidneys from the UUO model through immunofluorescence (A and B). Representative images from control and UUO kidneys (×200 magnification) are shown. The levels of TG2 (C) and TG ISA (D) were quantified by multiphase analysis; TG2 was quantified by dividing TG2 signal for DAPI, while TG ISA by dividing incorporated Texas red cadaverine by tissue area (green autofluorescence). All data were normalized by the WT control at day 7 UUO; the original values were 0.098 for TG2 and 3.564 for TG ISA. *$P<0.05$ versus control; †$P<0.05$ versus Sdc4 KO UUO.

basement membrane collagen IV transcript in the UUO mice and AAI-treated mice compared with the controls. There was a lower expression level in the Sdc4-KO mice, which was significant for collagen $\alpha 1$(I), III, and IV in the AAN model but reached significance only for collagen $\alpha 1$(I) in the UUO model (Supplemental Figure 1). Therefore, the knockout of Sdc4 caused a reduction in the development of kidney fibrosis in both models, and this was principally due to less deposited collagen.

The kidney weight to body weight ratio was lower in AAN but was preserved in the Sdc4-KO mice (Supplemental Figure 2A). Serum creatinine and creatinine clearance were respectively increased and decreased ($P<0.05$) in response to AAI but with no difference between the two genotypes. However, in this model, loss in function was higher at 9 weeks when only an early level of fibrosis was seen (Figure 3F), than after 12 weeks when fibrosis was more advanced (Supplemental Figure 2, B and C).

Sdc4-KO Lowers Extracellular TG2 in Two Mouse Models of CKD

The link between TG2 externalization and tubulointerstitial fibrosis is well known,[1] being associated with post-translational modification of the ECM and the recruitment of large latent TGF-$\beta 1$ that facilitates its activation.[6,8,9,33,34] Therefore, we examined the consequences of Sdc4-KO on extracellular TG2 in normal and diseased kidneys. Extracellular TG2 antigen was specifically detected on unfixed cryosections after washout of the intracellular enzyme.[1,12] Extracellular TG2 was mainly localized in the tubulointerstitial space and within the glomerular tuft (most likely within the mesangial matrix and glomerular basement membrane) in normal kidneys from WT and Sdc4-KO mice, with no quantitative difference in the level of extracellular TG2 between WT and Sdc4-KO control mice (Figures 4 and 5). In the UUO model, the levels of TG2 increased with the progression of kidney fibrosis in the tubulointerstitium, with the WT kidneys having significantly more extracellular TG2 than the Sdc4-KO kidneys at 14 and 21 days after UUO (Figure 4, A and C, Supplemental Figure 3).

In a manner similar to that seen in the UUO, there was progressive accumulation of extracellular TG2 in response to AAI (Figure 5A). Again, the level of externalized TG2 was significantly higher in the WT animals than in the Sdc4-null mice in the AAI-treated mice at 12 weeks (Figure 5, A

and C). Extracellular TG activity (Figures 4B and 5B) mirrored the distribution of TG2 antigen, with no quantitative difference in level between WT and Sdc4-KO control kidneys. UUO and AAN kidneys had a significantly higher level of TG activity at all the time points compared with the relative controls (Figures 4D and 5D). In the UUO, although mean extracellular TG activity was always higher in WT than in Sdc4-KO kidneys, this difference reached significance from day 14 (Figure 4D). In the AAN, extracellular TG activity was higher in WT than in Sdc4-KO kidneys at 12 weeks (Figure 5D). Western blot analysis of total homogenates revealed no differences in TG2 expression between the two genotypes (WT and Sdc4-KO) in control and diseased kidneys (Figure 6). This rules out the possibility that the lower extracellular TG2 detected in the Sdc4-KO kidneys that underwent experimental fibrosis was due to any difference in TG2 production between the two genotypes. Therefore, TG2 was elevated outside the cell in both models (Figures 4 and 5) through an increase in cellular
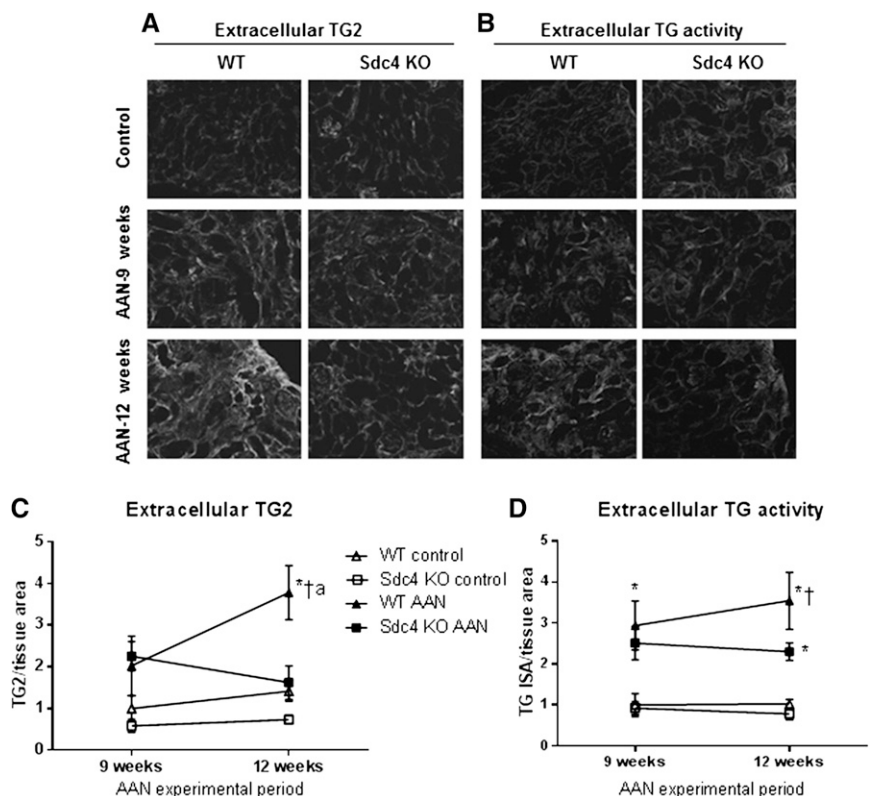

Figure 5. Sdc4-KO decreases extracellular TG2 and TG activity in the AAN model of CKD. Extracellular TG2 was detected using cryostat section of WT and Sdc4-KO kidneys from the AAN model through immunofluorescence (A). TG in situ activity was measured by incorporation of biointylated cadaverine revealed by TexasRed-labeled streptavidin (B). Quantification of levels of TG2 (C) and TG in situ activity (D) were performed using multiphase image analysis by dividing incorporated TG2 or TG activity by tissue area (green autofluorescence). All data were normalized by the WT control at week 9; the original values were 0.04 for TG2 and 0.03 for TG in situ activity. *$P<0.05$ compared to control; †$P<0.05$ compared to Sdc4-KO AAN; [a]changes from 9 and 12 weeks in the WT AAN groups.
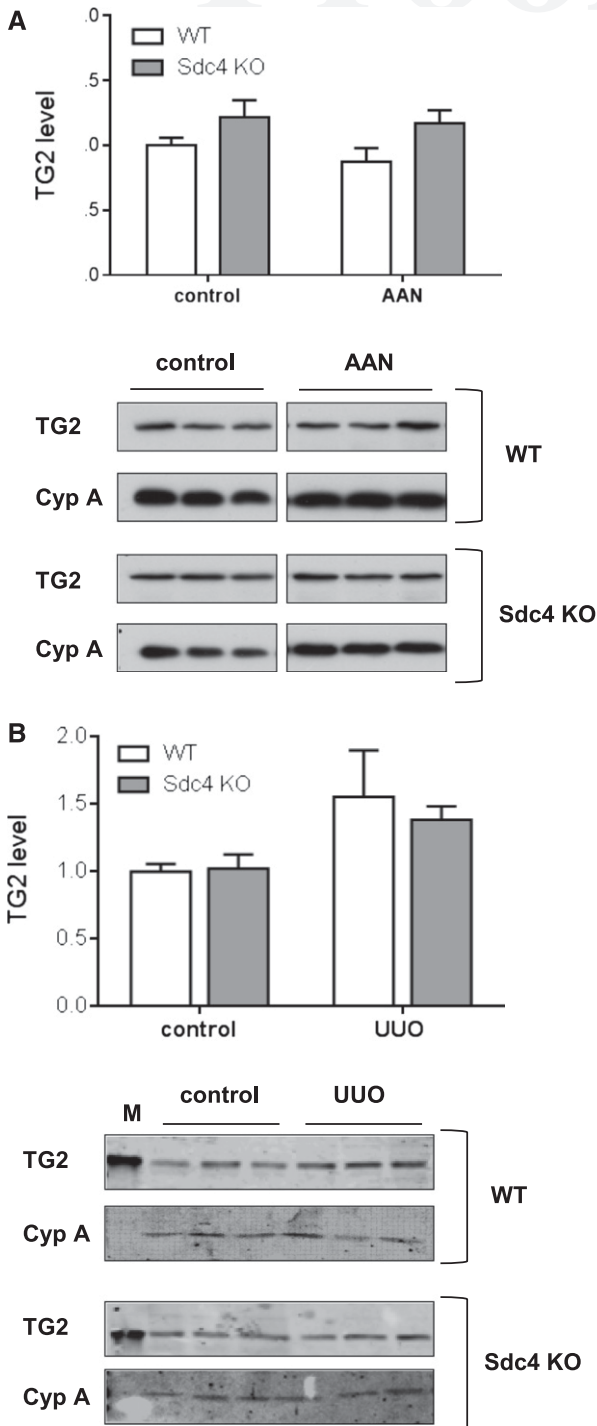
Figure 6. The expression of TG2 in kidney is similar in the WT and Sdc4-KO genotype. TG2 expression was evaluated by Western blot in control kidneys and fibrotic kidneys (total homogenates) from WT and Sdc4 KO mice. (A) AAN model. (B) UUO model. Cyclophilin A (Cyp A) was used as loading control. Twenty-five micrograms of kidney proteins was used, and 100 ng guinea pig liver TG2 was loaded as a control (M). TG2 protein level is expressed as mean±SEM of TG2/Cyp A (TG2 level); data are normalized for WT control. Differences in TG2 between the two genotypes and treatments were nonsignificant ($P>0.05$).

trafficking, rather than an upregulation *per se*, which was deficient in Sdc4-KO diseased kidneys.

Because TG2 was not found in the ECM of Sdc4-KO fibrotic kidney sections to the same extent as in the ECM of WT diseased kidneys, we analyzed whether it was retained intracellularly or in the cytosol. WT and Sdc4-KO fibrotic kidneys were fractionated into cytosol and membrane fractions, and equal loading of protein fractions was analyzed by Western blotting for TG2 expression. Sdc4-KO membrane fractions contained significantly less TG2 antigen than did the WT membrane fractions (Figure 7, A and D). Conversely, the Sdc4-KO cytosolic fractions had a higher amount of TG2 antigen compared with the WT (Figure 7, B and D). The combined level of TG2 was not significantly different in the two genotypes (Figure 7, C and D). We next visualized intracellular TG2 in paraffin sections, where ECM TG2 cannot be detected.[1,12] Compared with the WT fibrotic kidneys, staining of Sdc4-KO sections revealed an increase in cytosolic TG2 that was paralleled by a lower level of externalized TG2 after UUO, as specifically detected in cryostat sections (Figure 7E).[12] This finding is consistent with our prior data that Sdc4-null cells had an increased retention of TG2 inside the cell.[22] Therefore, Sdc4 influences the externalization of profibrotic TG2.

Extracellular TG2 Availability in the Renal Interstitium Depends on Binding to HSPG

To investigate the mechanism of Sdc4 modulation of TG2 externalization, we began with visualizing extracellular TG2 and Sdc4 in normal and fibrotic kidneys after AAI. Immunofluorescence analysis of unfixed cryostat sections revealed, in normal tissues, that Sdc4 and TG2 had mainly a tubular basement membrane localization; however, Scd4 staining was more diffuse and clearly outlined the perimeter of all cells of the renal interstitium, in keeping with its matrix cell-receptor role (Figure 8). In AAN kidneys, extracellular TG2 staining was more intense and filled the widened interstitial space, decorating the thickened basement membrane. Extracellular TG2 and Sdc4 clearly showed a parallel alignment with areas of intense extracellular TG2 staining lying adjacent to Sdc4 staining in AAN kidneys (Figure 8). Quantitative colocalization analysis according to Manders[35] indicated a good overlap coefficient (mean±SEM, 0.67±0.07 [1 is total colocalization]). The Pearson correlation coefficient was 0.64±0.04. The partial overlap and location in immediately adjacent regions, especially in the basement membrane, suggested that TG2 association with Sdc-4 could be mediated by the sulfated domains within HS chains, rather than the HSPG core protein. Syndecans are characterized by three to five GAG chains,[36] which typically vary in length and size, extending extensively in the extracellular space. Dual staining of extracellular TG2 and HS in sections from control and AAN kidneys (Figure 9) showed that HS were strongly expressed in the tubulointerstitium and were prominent in the basement membranes of the diseased kidney, where HS largely colocalized with TG2. Quantitative colocalization indicated an improved overlap coefficient
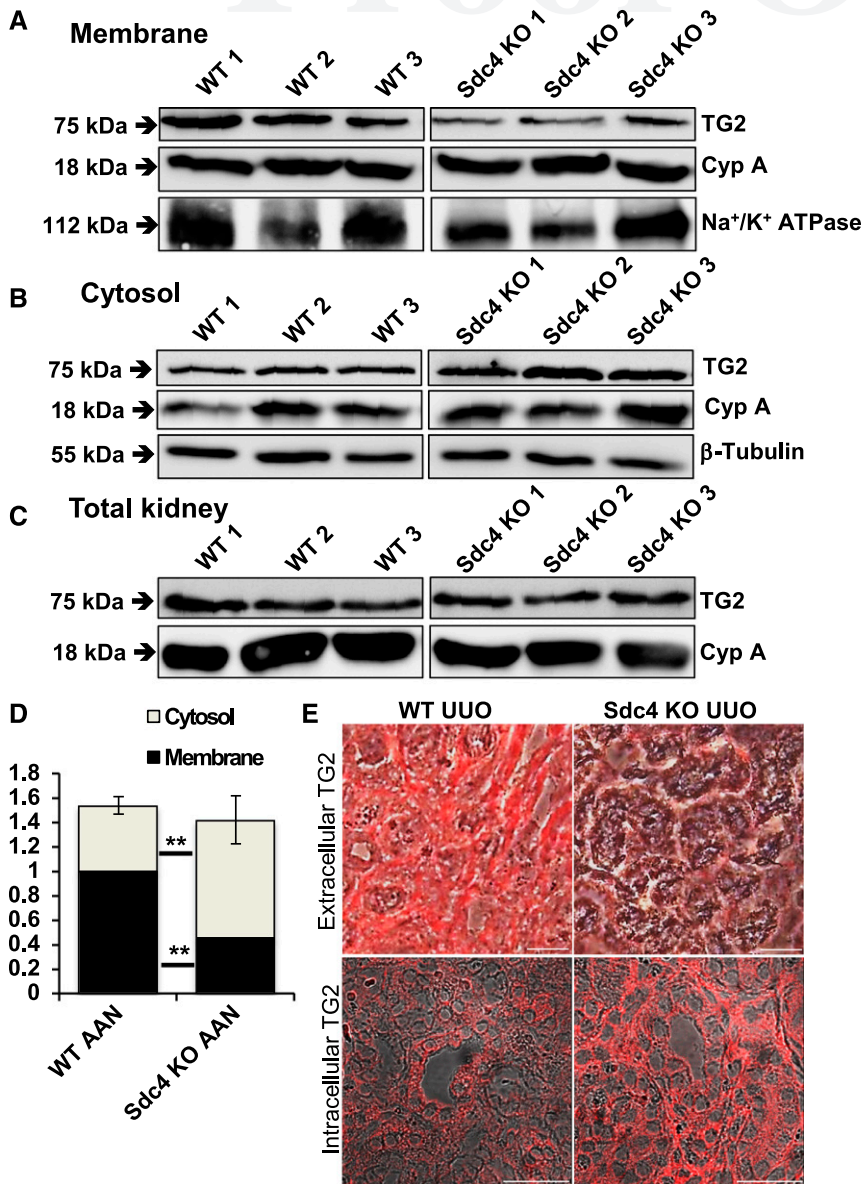
Figure 7. Sdc4-KO reduces the cell membrane targeting of TG2. TG2 expression was quantified by Western blot in the AAN kidneys from WT and Sdc4 KO mice (A–D). Kidney homogenates were fractionated as described in the Supplemental Methods. Forty-micrograms of kidney proteins was loaded. Cyclophilin A (Cyp A) was used as loading control, and β-tubulin and Na$^+$/K$^+$ ATPase were used as cytosolic and membrane markers, respectively. TG2 protein level is expressed as mean±SEM of TG2/Cyp A (TG2 level); data are normalized for WT membrane fraction. *$P<0.05$. (D). Extracellular TG2 was detected in cryosections and intracellular TG2 was immunostained in paraffin sections through immunofluorescence. Details of representative images of extracellular TG2 staining (Supplemental Figure 3) and representative images of intracellular TG2 overlapped to phase contrast at day 21 after UUO are shown at ×400 and ×630 magnification, respectively (E). Scale, 50 μm.

(0.85 ± 0.09) and Pearson correlation coefficient (0.77 ± 0.08). To confirm that TG2-association with the interstitial matrix depended on binding to the HS chains of proteoglycans, sections were preincubated with heparitinase I to selectively

cleave HS (Figure 10). Following heparitinase I pretreatment, both the interstitial space and the basement membrane were almost completely devoid of TG2 binding, indicating that HS plays a critical role in the cell-surface availability of TG2 (Figure 10).

Because we showed that Sdc-4 is critical to the availability of cell-surface TG2 in the diseased kidney (Figures 4 and 5), these findings suggest a role for the Sdc4-HS chains in recruiting TG2 at the basolateral membrane and the renal interstitium in progressive kidney fibrosis. HS not only characterized membrane HSPG but also secreted proteoglycans.[37] It would be reasonable to think that once TG2 is externalized in the renal interstitium, through the critical involvement of transmembrane Sdc4, it may be trafficked in the matrix by binding to basement membrane HSPG.

Sdc4-KO Reduces TGF-β1 Activation

Given that TG2 is involved in the activation of TGF-β1 by recruiting large latent TGF-β complex,[6,9,33,34] and failure to localize/recruit latent TGF-β1 results in altered TGF-β1 activity, the level of active TGF-β1 was evaluated through the mink lung bioassay (Figure 11).[34,38] Active TGF-β1 was similar in WT and Sdc-4 KO control kidneys. Active TGF-β1 was increased in the fibrotic kidneys of WT mice at 12 weeks of AAI treatment compared with controls but was not elevated to the same extent in the Sdc4-KO AAI-treated kidneys (Figure 11A). Total TGF-β1 was also significantly elevated in the fibrotic WT kidneys and not in the Sdc4-KO kidneys (Figure 11B). Overall, the percentage of active TGF-β1 in the WT AAI-treated kidneys was significantly higher than in the Sdc4-KO AAI-treated kidneys (Figure 11C). Syndecan-2 (Sdc2), the main syndecan protein found to directly interact with TGF-β1,[39] was not differently expressed in the Sdc4-KO normal and diseased kidneys compared with WT counterparts (Supplemental Figure 2). Therefore, we have confirmed a reduction in TGF-β1 activity associated with Sdc4 deletion.
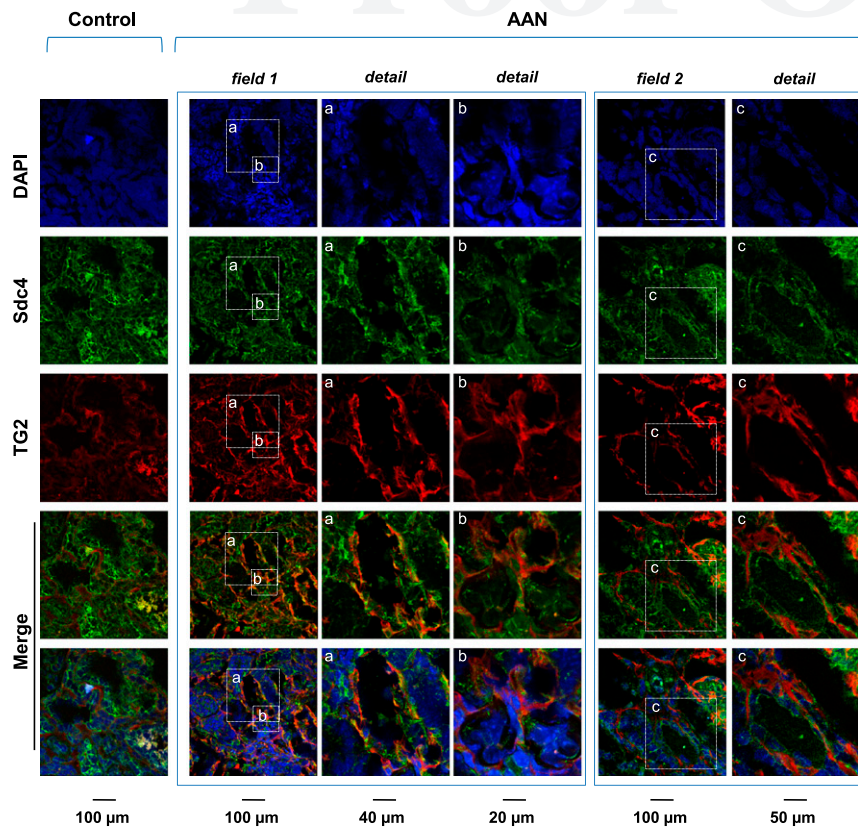
Figure 8. TG2 partially colocalize with Sdc4 core protein in tubulointerstitial fibrotic lesions. Sdc4 and TG2 immunostaining of cryostat sections was performed by using rabbit polyclonal anti-Sdc4 and mouse monoclonal anti-TG2 IA12 antibody followed by, respectively, donkey antirabbit AlexaFluor 488 and goat antimouse DyLight 594. Representative confocal images of Sdc4, TG2, and DAPI stained sections are shown separately and merged (with and without DAPI staining) for control and AAI-treated kidneys (two fibrotic lesions are shown, field 1 and field 2). Basolateral membrane localization of Sdc4 and TG2 after AAI is shown at higher magnification (details a, b, and c). Dual staining controls were carried out in kidney sections from TG2 KO and Sdc4 KO mice (Supplemental Figure 3). Scale bars are shown under each column of images.

DISCUSSION

All types of CKD progress to kidney failure through the common pathway of kidney fibrosis and scarring. Therefore, understanding the mechanisms involved in this is essential for the development of antifibrotic therapies. Studies have repeatedly highlighted the benefit of TG2 modulation on the progression of kidney fibrosis, but the tightly conserved catalytic triad within the TG family prevents the design of specific small-molecule TG2 inhibitors. In this paper, we have exploited recent *in vitro* observations that Sdc4 may have an important role in TG2 export and retention of TG2 at the cell surface,[23,40,41] to see whether or not targeting the TG2-Sdc4 interaction may provide such an interventional step.

We have chosen to do these studies in two models of CKD in parallel in order to prevent concerns over any model-specific responses. UUO is a well established model for rodents that

allows the fibrotic state to be developed in a relatively short time without the use of exogenous toxins and the development of uremia.[42] Although obstruction of the urinary tract has clinical relevance,[43] the interstitial fibrosis of this model is not typical of most types of CKD. Therefore, we have also used the relatively new AAN model, which does provide a typical tubulointerstitial fibrosis.[31,32,44]

The results in both models were highly consistent with lower levels of fibrosis detected in the Sdc4-KO animals, suggesting a protective role for Sdc4-KO in kidney fibrosis. Because fibrosis is an abnormal tissue repair process, this result fits with the involvement of Sdc4 in wound healing and the reported delay in wound repair in Sdc4-KO mice.[45,46]

Although, to our knowledge, this is the first study in CKD using Sdc4-KO mice, Sdc4-KO was investigated in mice with unilateral nephrectomy.[47] Glomerulosclerosis was reported in Sdc4-KO male mice after and was attributed to the compensatory expression of Sdc2 and activation of TGF-β1.[47] However, unilateral nephrectomy typically causes renal hypertrophy rather than overt fibrosis and, subsequently, is not similar to the two CKD models used here. Moreover, we did not see Sdc2 compensation in Sdc4-KO mice after UUO.

Extracellular TG activity positively correlated with fibrosis development in the two experimental models of renal fibrosis. To establish whether or not the protective effect of Sdc4-KO was related to its previously reported role in TG2 trafficking/cell-surface localization,[23,41] tissues were subjected to assays for both extracellular TG2 antigen and *in situ* TG activity. In both models, increased extracellular TG2 and TG activity was found to be in the same interstitial and periglomerular regions where increased collagen deposition was detected. Importantly, the increase in extracellular TG2 occurred in parallel with fibrosis, being significantly lower in the Sdc4-KO diseased animals. Because the total TG2 level was similar in both WT and Sdc4-null mice, the difference in TG2 antigen outside the cell could only be due to Sdc4 affecting the cell-surface availability of TG2. This conclusion was corroborated by the finding of reduced distribution of TG2 to the membrane and a higher proportion of cytosolic TG2 following Sdc4 silencing in kidney, consistent with similar findings in dermal fibroblasts from Sdc-4 KO mice.[23] Taken together, the *in vivo* and *ex vivo* data strongly support the hypothesis that Sdc4 plays a significant role in TG2 export and
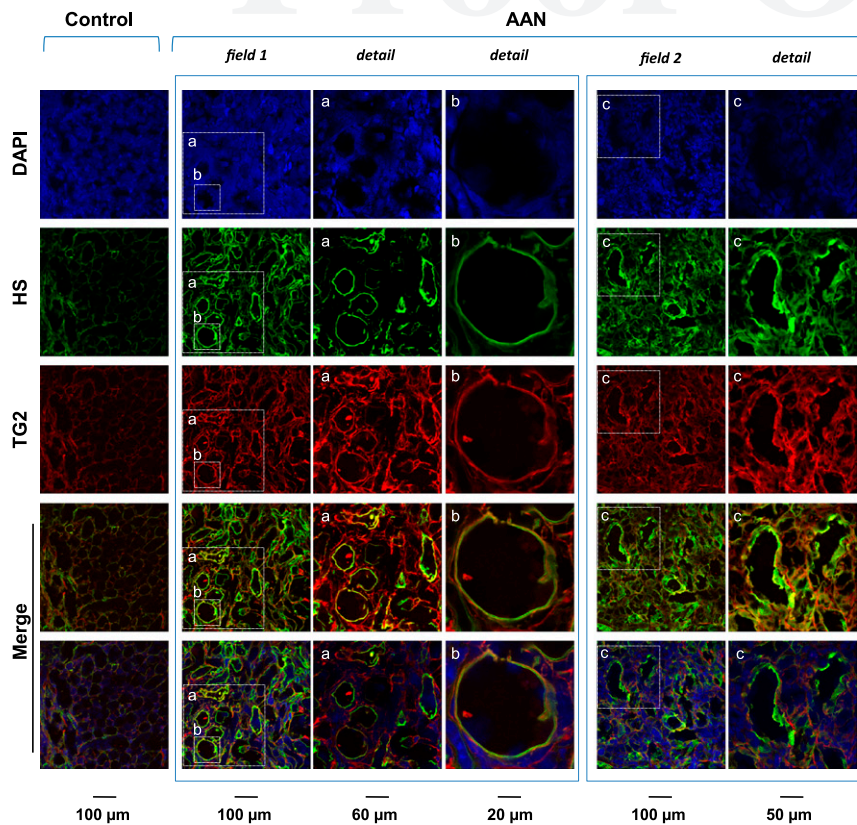
Figure 9. TG2 largely colocalize with HS chains in tubulointerstitial fibrotic lesions. HS and TG2 immunostaining of cryostat sections was performed using mouse monoclonal anti-HS antibody and rabbit polyclonal anti-TG2 antibody, followed by, respectively, goat anti-mouse (IgM) FITC and donkey anti-rabbit IgG AlexaFluor 568. Representative pictures of HS, TG2, and DAPI-stained sections are shown separately and merged (with and without DAPI staining) for control and AAI-treated kidneys (two fibrotic lesions are shown). Basolateral membrane and interstitial localization of HS and TG2 after AAI are shown at higher magnification (details a, b, and c). Dual staining controls were carried out in TG2 KO kidney sections (Supplemental Figure 3). Scale bars are shown under each column of images.

activated by the increased calcium ions and low guanine nucleotides,[10] leading to matrix stabilization by crosslinking of fibronectin and collagen. Although not tested, it is conceivable to speculate that further diffusion of TG2 from the cell surface may be regulated by shedding of TG2-Sdc4 from the cell surface by matrix metalloproteases, which are abundant, into a wound healing/fibrotic context. Furthermore, the HS chains could facilitate diffusion of TG2 through dissociation/reassociation *via* adjacent binding sites, thus allowing TG2 to "slide" in the matrix, depending on the specificity of the HS interaction. The significant but partial attenuation of extracellular TG2 activity and export in two Sdc4-KO mice models of CKD, and its complete abolishment by digestion of the HS chains, suggest that additional HSPG may be implicated in TG2 localization in the renal interstitium. Secreted proteoglycans, such as perlecan, agrin, and collagen VIII (typical glomerular basement membrane proteoglycans), are also expressed in the tubule interstitium.[37] Taken together, our finding suggests that TG2 cell-surface availability may depend on trapping of TG2 by the HS chains of transmembrane HSPG Sdc4. Further engagement of TG2 with basement membrane–secreted HSPG may facilitate the distribution of extracellular TG2 into the matrix.

Our findings support the idea that Sdc4 and TG2 cooperate in the fibrotic process and Sdc4-KO reduces fibrosis through this route. In addition to controlling the cell-surface availability and function of extracellular TG2, Sdc4 regulates the export of other fibrogenic factors, such as fibroblast growth factor-2.[25] Sdc4/HS have also been shown to influence and integrate the procontractile signals from TGF-β1, leading to increased cell adhesion during scarring,[48] and trapping of exogenously provided TGF-β.[49] TG2 participates in the TGF-β1 recruitment/activation cascade by crosslinking the amino-terminal region of LTBP-1 to ECM proteins (diagram c in Figure 12).[6,33,50] This, together with matrix accumulation and stabilization by direct post-translational modification of ECM proteins (diagram b in Figure 12), is accountable for the fibrotic role of TG2 *in vivo*.[8,34] Of note, we found the protective role of Sdc4-KO on fibrosis to be associated with lower activation of TGF-β1. This is predictable given the lower TG2 activity in the ECM. The TG2-KO mouse is protected against kidney UUO-induced fibrosis[8] and pulmonary fibrosis,[7] and this is due partly to lower levels of profibrotic active TGF-β1 in the damaged

localization and that interference with TG2-Sdc4 interaction may have therapeutic value.

In the tubular epithelial cell line NRK-52E, we previously reported that TG2 is transported basolaterally into the tubular basement membrane through an unconventional pathway, most likely linked to direct molecular trap involving transmembrane transport.[21] Here we have shown for the first time that HS are critical for extracellular TG2 association with the tubular basement membrane. Therefore, TG2 is likely to be "trapped" by HS as soon as secreted from the plasma membrane (diagram a in Figure 12). The components required for TG2-membrane translocation are unknown, but the membrane-proximal HS chains of Sdc4 are a key factor. TG2 is a high-affinity ligand for heparin/HS with a dissociation constant in the low nanomolar range,[22] and folding of TG2 forms a functional heparin-binding domain.[24] Upon injury-induced tissue damage, the externalized TG2 is thought to be
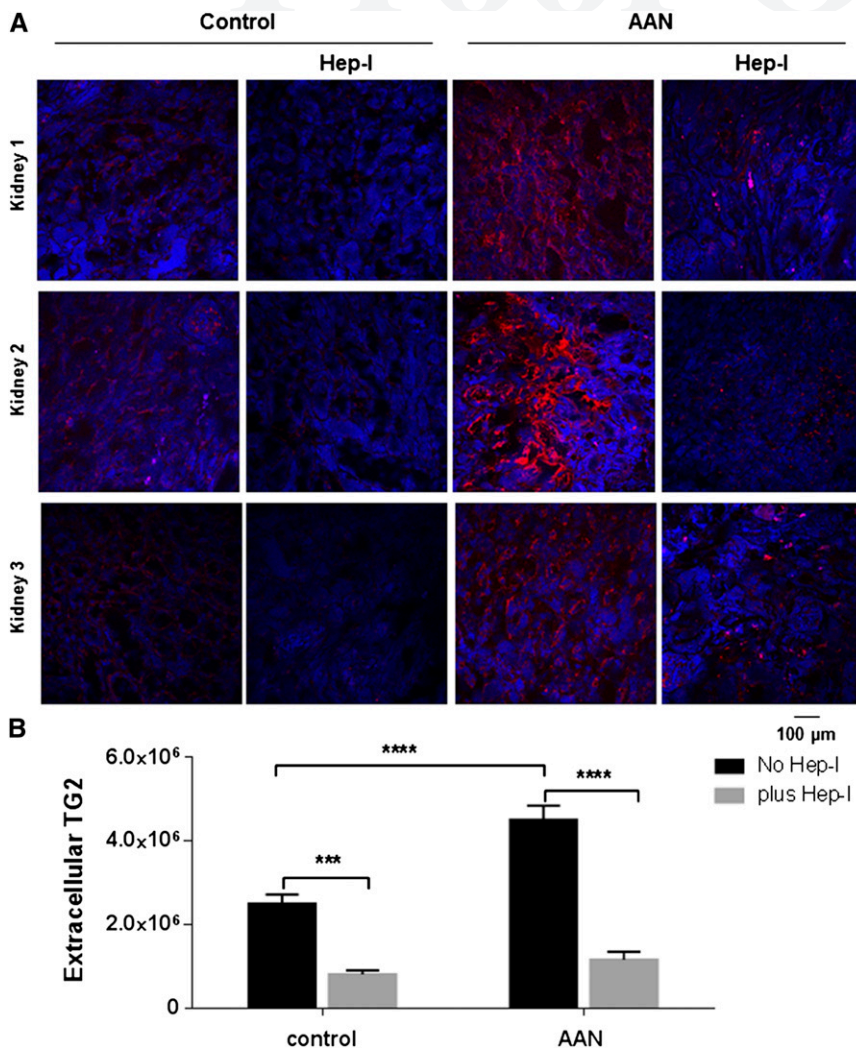
Figure 10. TG2 extracellular location depends on the HS chains of HSPGs. Kidney cryosections were treated with 50 mU/ml protease-free heparitinase I (Hep-I) for 2 hours at 37°C. Extracellular TG2 was immunolabeled using mouse anti-TG2 IA12 antibody followed by goat anti-mouse DyLight 594. Images were obtained by confocal microscopy (A) and the level of extracellular TG2 was quantified by ImageJ intensity analysis in four kidneys per treatment (B). Three fields are shown per treatment, representative of control and AAN fibrotic kidneys (A).

A surprising finding in this study is that although Sdc4-KO is clearly protective, with strong reduction in fibrosis in both models of kidney fibrosis, this did not have a knock-on effect on kidney function in the AAN model. The most obvious explanation is that the AAN is primarily a model of tubulointerstitial fibrosis. At 12 weeks, there was only minimal glomerulosclerosis because the disease had not gained glomerular involvement at this stage. It is therefore not surprising that there was no effect on glomerular filtration. This raises the question as to why both WT and Sdc4-KO animals treated with AAI had elevated serum creatinine and lower clearance at both time points. In rodents and mice especially, creatinine is secreted from the tubules and because AAI is cytotoxic to the tubular epithelial cells; this would clearly interfere with creatinine excretion through this route. Thus, because serum creatinine decreased from 9 to 12 weeks, this simply reflected the epithelial cell recovery to AAI toxicity, which undoubtedly masked any early fibrotic changes on kidney function due to fibrosis.

In conclusion, Sdc4-KO is protective in two models of tubulointerstitial fibrosis. In both cases this is related to a reduction of extracellular TG2 antigen and activity, which has previously been shown to be a primary cause of scar tissue formation in renal fibrosis by both direct post-translational modification and indirect TGF-β1 recruitment. Therefore, Sdc4 is involved in extracellular trafficking and cell-surface targeting of profibrogenic TG2 *in vivo*. These data may ultimately be useful in designing interventional strategies for CKD.

organ or bronchoalveolar lavage, respectively.[7] Given that Sdc4-KO leads to lower extracellular TG2, which is needed for one of the three known mechanisms of TGF-β1 recruitment and activation[51] then it is reasonable to suggest that the lower active TGF-β1 is affected by impaired TG2 recruitment of the LTBP. Although a direct role of Sdc4 in TGF-β1 activation has not been reported, the ability of Sdc4 to act as a reservoir of growth factors leaves open the possibility of a synergistic action between TG2 and Sdc4 in TGF-β1 activation (diagram d in Figure 12). Therefore, because Sdc4 and TG2 affect multiple pathways in the fibrotic program, targeting the TG2-Sdc4 interaction, would probably form part of a multifaceted interventional strategy against fibrosis.

CONCISE METHODS

Experimental Models

Experimental UUO was performed on Sdc4-KO[29] and control C57BL/6J mice. Anesthesia was induced with 5% fluorothane and maintained by 2% fluorothane during the surgical process, wherein the left ureter of each animal was blocked with a legating clip (Hemoclip Plus; Weck Closure Systems). The peritoneum was flooded with ADEPT (4% icodextrin solution) to prevent postsurgical adhesions before closing. The muscle wall was closed with single crossover stitching using dissolvable stitches. After UUO, mice were provided with buprenorphine (0.1 mg/kg) for 40 hours for analgesic purposes.
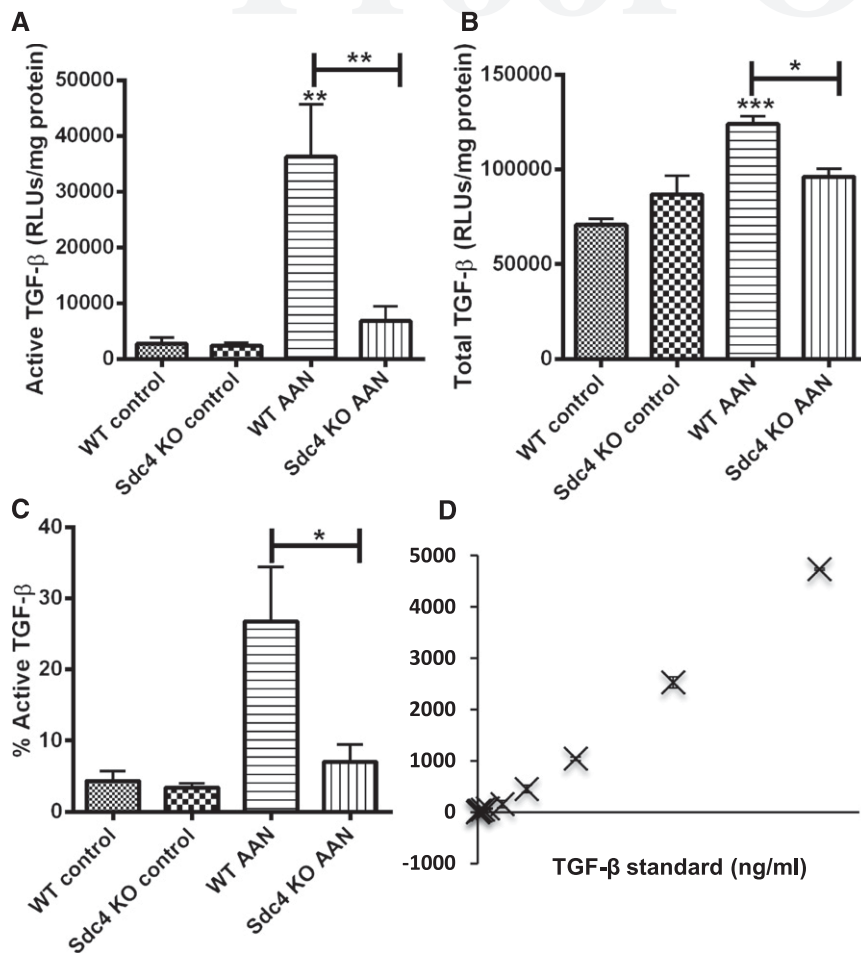
Figure 11. Sdc4-KO lowers TGF-β1 in the AAN model of CKD. Active TGF-β (A), total TGF-β (B), and percentage of activated TGF-β (C) were evaluated in WT and Sdc4-KO kidneys using the mink lung TGF-β bioassay, as described in the Concise Methods.[38] Total TGF-β was converted to a biologically active form for analysis by acid activation. The percentage of activation was calculated by expressing the level of active TGF-β as a percentage of total TGF-β. (D) Recombinant TGF-β standard curve. Values are the mean of four kidneys$\pm$SEM, each assessed in triplicate. RLU, relative light unit. *$P<0.05$ compared with the control or compared with Sdc4 KO AAN.

Kidney Function

Terminal blood samples were taken. Twenty-four-hour urine samples were collected using metabolic cages 24 hours before termination. Serum and urine creatinine was measured as previously described,[32,50] with modifications detailed in the Supplemental Methods.

Fibrosis Measurement

Kidney fibrosis was assessed on kidney sections stained with MT as previously described.[32,50] To assess the scarring index in the UUO study, 10 images per kidney were acquired at $\times 200$ magnification. For the AAN model, the measurement was performed using images acquired at $\times 100$ magnification along the whole cortical area of each kidney.

Immunohistochemistry

Immunodetection of collagens was performed on 4-μm paraffin sections. After antigen retrieval and blocking, sections were incubated with primary antibodies against collagen I (rabbit anticollagen I; Abcam; 1:250) collagen III (goat anticollagen III; Southern Biotech; 1:10) or collagen IV (rabbit antihuman collagen IV; MP Biomedicals; 1:35). AlexaFluor 568 (UUO model) or AlexaFluor 488 (AAN model) secondary antibodies (Invitrogen; 1:200) were used for the immunofluorescent staining, and coverslips were mounted with 4',6-diamidino-2-phenylindole (DAPI)-containing Vectashield (Vectorlab). Ten nonoverlapping images of the cortical regions were acquired at $\times 200$ magnification and analyzed using multiphase image analysis with correction to DAPI staining.

Immunodetection of extracellular TG2 was performed on 14-μm-thick cryostat sections, as previously described by Johnson *et al.* in 1999 and 2003[1,12] and reported in the Supplemental Methods. We used mouse monoclonal anti-TG2 (clone ID10; Abcam; 1:100) followed by goat anti-mouse AlexaFluor 568 (Invitrogen; 1:200), or mouse anti-TG2 monoclonal IA12 (University of Sheffield; 1:100), followed by goat anti-mouse IgG DyLight 594 (Abcam; 1:200). Coverslips were mounted with DAPI-containing Vectashield. For TG2 quantification, ten $\times 200$ pictures of the cortical region were acquired for each kidney and analyzed as described above.

TG2 and Sdc4 double staining was performed using rabbit polyclonal anti-Sdc4 (Zymed; 1:50) and mouse anti-TG2 IgG monoclonal IA12 (University of Sheffield, United Kingdom; 1:100) followed by donkey anti-rabbit IgG AlexaFluor 488 (Invitrogen; 1:200) and goat anti-mouse IgG DyLight 594 (Abcam; 1:200). HS and TG2 dual staining was performed using mouse IgM anti-HS antibody (Amsbio, 1:50) and rabbit polyclonal anti-TG2 (Abcam, 1:50) followed by goat anti-mouse IgM FITC (Sigma-Aldrich; 1:100) and

Mice were allowed to recover and had free access to food and water. Kidneys were harvested at days 7, 14, and 21 (Supplemental Table 1).

AAN was induced in 8-week-old male C57BL/6J and Sdc4-KO mice by intraperitoneal injection of AAI (Sigma-Aldrich).[52] Administration of AAI, 3 mg/kg, once every 3 days for 3 or 6 weeks, as described in Supplemental Table 2, established progressive fibrosis.[32,50] Control animals received intraperitoneal injection of vehicle control DMSO (Sigma-Aldrich). Mice were maintained at 20°C and 45% humidity on a 12-hour light/dark cycle and allowed free access to standard rodent chow and water.

All procedures were carried out under license according to regulations laid down by Her Majesty's Government, United Kingdom (Animals Scientific Procedures Act, 1986).
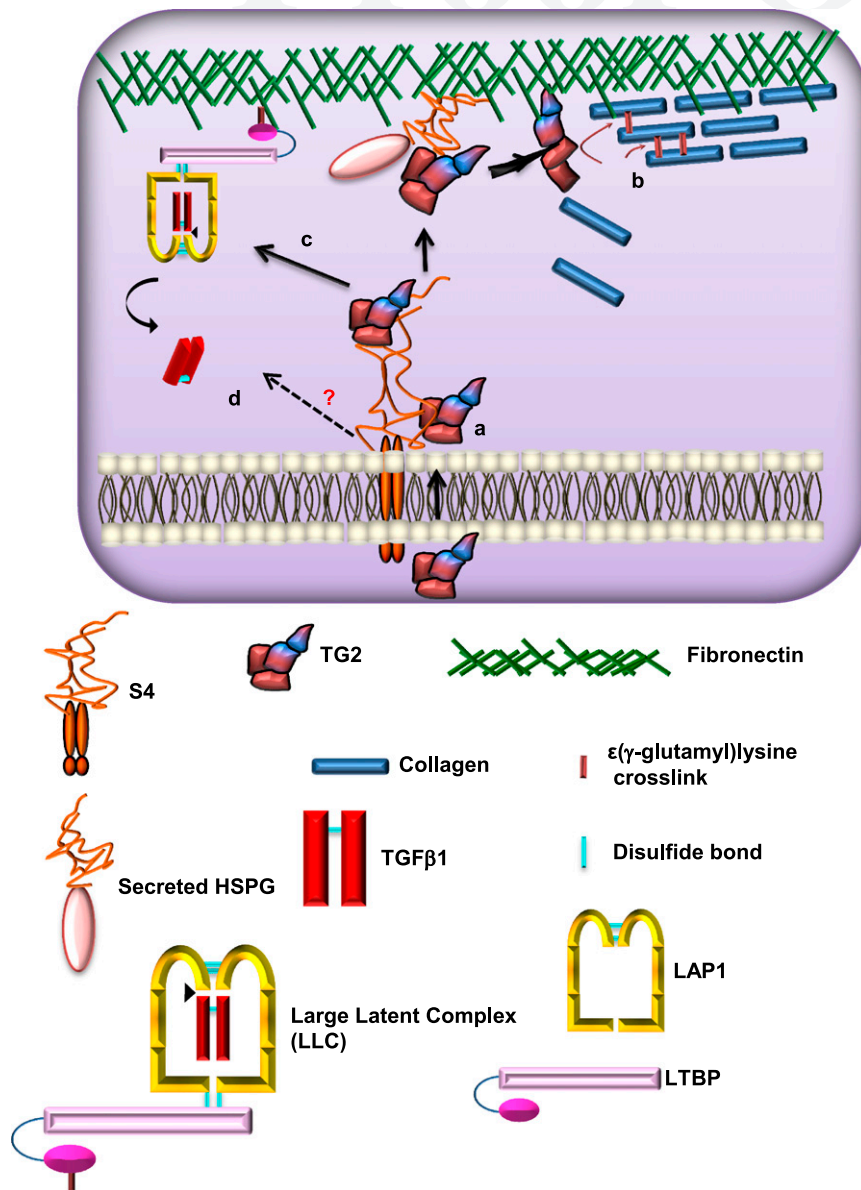
Figure 12. Interplay between TG2 and Sdc4/HS in TG2 externalization and matrix crosslinking during the development of fibrosis. Transmembrane Sdc4 traps TG2 at the cell surface through its HS chains, facilitating TG2 externalization. It is unclear how TG2 crosses the plasma membrane. The HS chains of secreted HSPG could facilitate diffusion of TG2 *via* adjacent binding sites, thus allowing TG2 to "slide" in the matrix (a). Engagement with protein substrates (collagen, fibronectin) leads to activation of TG2 transamidation, resulting in matrix stabilization by crosslinking (b). Furthermore, TG2 promotes TGF-β1 large latent complex (LLC) deposition into the ECM by covalently linking the latent TGF-β1–binding protein (LTBP) to matrix components (c),[6,33], leading to its activation in the fibrotic kidney.[8,9] TGF-β1 and the latency-associated peptide (LAP) are proteolytically separated at the site indicated by the arrowhead.[51] Sdc4 could trap LLC *via* HS chains and/or contribute to TGF-β1 activation directly or indirectly through other Sdc4-linked pathways (d).

donkey anti-rabbit IgG AlexaFluor 568 (Invitrogen; 1:200) in Tris-buffered saline with Tween-20 containing 1% vol/vol serum (donkey and goat). The dual staining protocol is described in the Supplemental

Methods. Images were captured using a Leica SP5 confocal microscope scanning system coupled to a ×40 and ×63 oil immersion objective-inverted microscope. Successive serial optical sections (0.5–1 μm) were recorded over a range of specimen planes (3–7 μm). Colocalization was estimated as described in Supplemental Methods.

Enzymatic Pretreatment

Proteinase-free heparitinase I (EC 4.2.2.8) (Sigma-Aldrich) was used to digest the side chains of HSPG. Enzymatic pretreatments of cryosections were performed with heparitinase I (0.05 U/ml) dissolved according to the manufacturer's instructions and incubated for 2 hours at 37°C.[53] TG2 was detected by immunofluorescence as described earlier. Extracellular TG2 was quantified using the WCIF ImageJ integrated density tool, which is a measure of pixel intensity. All images were processed for background noise subtraction before analysis for intensity. Four kidneys were analyzed per treatment (approximately three sections per kidney; four to seven nonoverlapping images per section).

Detection of TG *In Situ* Activity

In situ activity was detected as previously described by Huang and colleagues[26–28] using 0.1 mM Texas red cadaverine instead of biotinylated cadaverine. **Q:7**

TGF-β1 Activity

Active and total TGF-β1 were determined using the MLEC luciferase TGF-β quantitative bioassay as previously described.[38] Details are provided in the Supplemental Methods. **Q:8**

Statistical Analyses

Data are shown as mean±SEM. Data analyses were performed using two-way ANOVA followed by a Bonferroni *post hoc* test or a *t* test. A probability of 95% ($P<0.05$) was taken as indicating a statistically significant result.

DISCLOSURES

None.

REFERENCES

1. Johnson TS, El-Koraie AF, Skill NJ, Baddour NM, El Nahas AM, Njloma M, Adam AG, Griffin M: Tissue transglutaminase and the progression of human renal scarring. *J Am Soc Nephrol* 14: 2052–2062, 2003

2. Johnson TS, Fisher M, Haylor JL, Hau Z, Skill NJ, Jones R, Saint R, Coutts I, Vickers ME, El Nahas AM, Griffin M: Transglutaminase inhibition reduces fibrosis and preserves function in experimental chronic kidney disease. *J Am Soc Nephrol* 18: 3078–3088, 2007

3. Johnson TS, Haylor JL, Thomas GL, Fisher M, El Nahas AM: Matrix metalloproteinases and their inhibitions in experimental renal scarring. *Exp Nephrol* 10: 182–195, 2002

4. Skill NJ, Griffin M, El Nahas AM, Sanai T, Haylor JL, Fisher M, Jamie MF, Mould NN, Johnson TS: Increases in renal epsilon-(gamma-glutamyl)-lysine crosslinks result from compartment-specific changes in tissue transglutaminase in early experimental diabetic nephropathy: pathologic implications. *Lab Invest* 81: 705–716, 2001

5. Verderio EA, Johnson TS, Griffin M: Transglutaminases in wound healing and inflammation. *Prog Exp Tumor Res* 38: 89–114, 2005

6. Nunes I, Gleizes PE, Metz CN, Rifkin DB: Latent transforming growth factor-beta binding protein domains involved in activation and transglutaminase-dependent cross-linking of latent transforming growth factor-beta. *J Cell Biol* 136: 1151–1163, 1997

7. Oh K, Park HB, Byoun OJ, Shin DM, Jeong EM, Kim YW, Kim YS, Melino G, Kim IG, Lee DS: Epithelial transglutaminase 2 is needed for T cell interleukin-17 production and subsequent pulmonary inflammation and fibrosis in bleomycin-treated mice. *J Exp Med* 208: 1707–1719, 2011

8. Shweke N, Boulos N, Jouanneau C, Vandermeersch S, Melino G, Dussaule JC, Chatziantoniou C, Ronco P, Boffa JJ: Tissue transglutaminase contributes to interstitial renal fibrosis by favoring accumulation of fibrillar collagen through TGF-beta activation and cell infiltration. *Am J Pathol* 173: 631–642, 2008

9. Kojima S, Nara K, Rifkin DB: Requirement for transglutaminase in the activation of latent transforming growth factor-beta in bovine endothelial cells. *J Cell Biol* 121: 439–448, 1993

10. Lorand L, Graham RM: Transglutaminases: Crosslinking enzymes with pleiotropic functions. *Nat Rev Mol Cell Biol* 4: 140–156, 2003

11. Johnson TS, Griffin M, Thomas GL, Skill J, Cox A, Yang B, Nicholas B, Birckbichler PJ, Muchaneta-Kubara C, Meguid El Nahas A: The role of transglutaminase in the rat subtotal nephrectomy model of renal fibrosis. *J Clin Invest* 99: 2950–2960, 1997

12. Johnson TS, Skill NJ, El Nahas AM, Oldroyd SD, Thomas GL, Douthwaite JA, Haylor JL, Griffin M: Transglutaminase transcription and antigen translocation in experimental renal scarring. *J Am Soc Nephrol* 10: 2146–2157, 1999

13. El Nahas AM, Abo-Zenah H, Skill NJ, Bex S, Wild G, Griffin M, Johnson TS: Elevated epsilon-(gamma-glutamyl)lysine in human diabetic nephropathy results from increased expression and cellular release of tissue transglutaminase. *Nephron Clin Pract* 97: c108–c117, 2004

14. Mirza A, Liu SL, Frizell E, Zhu J, Maddukuri S, Martinez J, Davies P, Schwarting R, Norton P, Zern MA: A role for tissue transglutaminase in hepatic injury and fibrogenesis, and its regulation by NF-kappaB. *Am J Physiol* 272: G281–G288, 1997

15. Grenard P, Bresson-Hadni S, El Alaoui S, Chevallier M, Vuitton DA, Ricard-Blum S: Transglutaminase-mediated cross-linking is involved in the stabilization of extracellular matrix in human liver fibrosis. *J Hepatol* 35: 367–375, 2001

16. Johnson TS, Abo-Zenah H, Skill JN, Bex S, Wild G, Brown CB, Griffin M, El Nahas AM: Tissue transglutaminase: a mediator and predictor of chronic allograft nephropathy? *Transplantation* 77: 1667–1675, 2004

17. Verderio EA, Telci D, Okoye A, Melino G, Griffin M: A novel RGD-independent cel adhesion pathway mediated by fibronectin-bound tissue transglutaminase rescues cells from anoikis. *J Biol Chem* 278: 42604–42614, 2003

18. Telci D, Wang Z, Li X, Verderio EA, Humphries MJ, Baccarini M, Basaga H, Griffin M: Fibronectin-tissue transglutaminase matrix rescues RGD-impaired cell adhesion through syndecan-4 and beta1 integrin co-signaling. *J Biol Chem* 283: 20937–20947, 2008

19. Belkin AM: Extracellular TG2: Emerging functions and regulation. *FEBS J* 278: 4704–4716, 2011

20. Siegel M, Khosla C: Transglutaminase 2 inhibitors and their therapeutic role in disease states. *Pharmacol Ther* 115: 232–245, 2007

21. Zemskov EA, Mikhailenko I, Hsia RC, Zaritskaya L, Belkin AM: Unconventional secretion of tissue transglutaminase involves phospholipid-dependent delivery into recycling endosomes. *PLoS ONE* 6: e19414, 2011

22. Chou CY, Streets AJ, Watson PF, Huang L, Verderio EA, Johnson TS: A crucial sequence for transglutaminase type 2 extracellular trafficking in renal tubular epithelial cells lies in its N-terminal beta-sandwich domain. *J Biol Chem* 286: 27825–27835, 2011

23. Scarpellini A, Germack R, Lortat-Jacob H, Muramatsu T, Billett E, Johnson T, Verderio EA: Heparan sulfate proteoglycans are receptors for the cell-surface trafficking and biological activity of transglutaminase-2. *J Biol Chem* 284: 18411–18423, 2009

24. Lortat-Jacob H, Burhan I, Scarpellini A, Thomas A, Imberty A, Vivès RR, Johnson T, Gutierrez A, Verderio EA: Transglutaminase-2 interaction with heparin: Identification of a heparin binding site that regulates cell adhesion to fibronectin-transglutaminase-2 matrix. *J Biol Chem* 287: 18005–18017, 2012

25. Zehe C, Engling A, Wegehingel S, Schäfer T, Nickel W: Cell-surface heparan sulfate proteoglycans are essential components of the unconventional export machinery of FGF-2. *Proc Natl Acad Sci U S A* 103: 15479–15484, 2006

26. Clayton A, Thomas J, Thomas GJ, Davies M, Steadman R: Cell surface heparan sulfate proteoglycans control the response of renal interstitial fibroblasts to fibroblast growth factor-2. *Kidney Int* 59: 2084–2094, 2001

27. Yung S, Woods A, Chan TM, Davies M, Williams JD, Couchman JR: Syndecan-4 up-regulation in proliferative renal disease is related to microfilament organization. *FASEB J* 15: 1631–1633, 2001

28. Fan Q, Shike T, Shigihara T, Tanimoto M, Gohda T, Makita Y, Wang LN, Horikoshi S, Tomino Y: Gene expression profile in diabetic KK/Ta mice. *Kidney Int* 64: 1978–1985, 2003

29. Ishiguro K, Kadomatsu K, Kojima T, Muramatsu H, Tsuzuki S, Nakamura E, Kusugami K, Saito H, Muramatsu T: Syndecan-4 deficiency impairs focal adhesion formation only under restricted conditions. *J Biol Chem* 275: 5249–5252, 2000

30. Vielhauer V, Anders HJ, Mack M, Cihak J, Strutz F, Stangassinger M, Luckow B, Gröne HJ, Schlöndorff D: Obstructive nephropathy in the mouse: Progressive fibrosis correlates with tubulointerstitial chemokine expression and accumulation of CC chemokine receptor 2- and 5-positive leukocytes. *J Am Soc Nephrol* 12: 1173–1187, 2001

31. Debelle FD, Nortier JL, De Prez EG, Garbar CH, Vienne AR, Salmon IJ, Deschodt-Lanckman MM, Vanherweghem JL: Aristolochic acids induce chronic renal failure with interstitial fibrosis in salt-depleted rats. *J Am Soc Nephrol* 13: 431–436, 2002

32. Huang L, Scarpellini A, Funck M, Verderio EA, Johnson TS: Development of a chronic kidney disease model in C57BL/6 mice with relevance to human pathology. *Nephron Extra* 3: 12–29, 2013

33. Verderio E, Gaudry C, Gross S, Smith C, Downes S, Griffin M: Regulation of cell surface tissue transglutaminase: effects on matrix storage of latent transforming growth factor-beta binding protein-1. *J Histochem Cytochem* 47: 1417–1432, 1999

34. Huang L, Haylor JL, Fisher M, Hau Z, El Nahas AM, Griffin M, Johnson TS: Do changes in transglutaminase activity alter latent transforming growth factor beta activation in experimental diabetic nephropathy? *Nephrol Dial Transplant* 25: 3897–3910, 2010

Q:9

35. Manders EMM, Verbeek FJ, Aten JA: Measurement of colocalization of objects in dual-color confocal images. *J Microsc ~~Oxford~~* 169: 375–382, 1993

36. Sarrazin S, Lamanna WC, Esko JD: Heparan sulfate proteoglycans. *Cold Spring Harb Perspect Biol* 3: 3, 2011

37. Rienstra H, Katta K, Celie JW, van Goor H, Navis G, van den Born J, Hillebrands JL: Differential expression of proteoglycans in tissue remodeling and lymphangiogenesis after experimental renal transplantation in rats. *PLoS ONE* 5: e9095, 2010

38. Abe M, Harpel JG, Metz CN, Nunes I, Loskutoff DJ, Rifkin DB: An assay for transforming growth factor-beta using cells transfected with a plasminogen activator inhibitor-1 promoter-luciferase construct. *Anal Biochem* 216: 276–284, 1994

39. Chen L, Klass C, Woods A: Syndecan-2 regulates transforming growth factor-beta signaling. *J Biol Chem* 279: 15715–15718, 2004

40. Verderio EA, Scarpellini A, Johnson TS: Novel interactions of TG2 with heparan sulfate proteoglycans: Reflection on physiological implications. *Amino Acids* 36: 671–677, 2009

41. Seikaly MG, Ho PL, Emmett L, Fine RN, Tejani A: Chronic renal insufficiency in children: The 2001 Annual Report of the NAPRTCS. *Pediatr Nephrol* 18: 796–804, 2003

42. Schainuck LI, Striker GE, Cutler RE, Benditt EP: Structural-functional correlations in renal disease. II. The correlations. *Hum Pathol* 1: 631–641, 1970

43. Fragiadaki M, Witherden AS, Kaneko T, Sonnylal S, Pusey CD, Bou-Gharios G, Mason RM: Interstitial fibrosis is associated with increased COL1A2 transcription in AA-injured renal tubular epithelial cells in vivo. *Matrix Biol* 30: 396–403, 2011

44. Echtermeyer F, Streit M, Wilcox-Adelman S, Saoncella S, Denhez F, Detmar M, Goetinck P: Delayed wound repair and impaired angiogenesis in mice lacking syndecan-4. *J Clin Invest* 107: R9–R14, 2001

45. Bishop JR, Schuksz M, Esko JD: Heparan sulphate proteoglycans fine-tune mammalian physiology. *Nature* 446: 1030–1037, 2007

46. Cevikbas F, Schaefer L, Uhlig P, Robenek H, Theilmeier G, Echtermeyer F, Bruckner P: Unilateral nephrectomy leads to up-regulation of syndecan-2- and TGF-beta-mediated glomerulosclerosis in syndecan-4 deficient male mice. *Matrix Biol* 27: 42–52, 2008

47. Wang Z, Collighan RJ, Pytel K, Rathbone DL, Li X, Griffin M: Characterization of heparin-binding site of tissue transglutaminase: Its importance in cell surface targeting, matrix deposition, and cell signaling. *J Biol Chem* 287: 13063–13083, 2012

48. Chen Y, Shi-Wen X, van Beek J, Kennedy L, McLeod M, Renzoni EA, Bou-Gharios G, Wilcox-Adelman S, Goetinck PF, Eastwood M, Black CM, Abraham DJ, Leask A: Matrix contraction by dermal fibroblasts requires transforming growth factor-beta/activin-linked kinase 5, heparan sulfate-containing proteoglycans, and MEK/ERK: insights into pathological scarring in chronic fibrotic disease. *Am J Pathol* 167: 1699–1711, 2005

49. Ishiguro K, Kadomatsu K, Kojima T, Muramatsu H, Iwase M, Yoshikai Y, Yanada M, Yamamoto K, Matsushita T, Nishimura M, Kusugami K, Saito H, Muramatsu T: Syndecan-4 deficiency leads to high mortality of lipopolysaccharide-injected mice. *J Biol Chem* 276: 47483–47488, 2001

50. Huang L, Johnson TS: Development of a chronic kidney disease model in C57BL/6 mice that is relevant to human disease. Presented at the BRS/RA Conference, Birmingham, United Kingdom, June 6, 2011.

51. Annes JP, Munger JS, Rifkin DB: Making sense of latent TGFbeta activation. *J Cell Sci* 116: 217–224, 2003

52. Sato N, Takahashi D, Chen SM, Tsuchiya R, Mukoyama T, Yamagata S, Ogawa M, Yoshida M, Kondo S, Satoh N, Ueda S: Acute nephrotoxicity of aristolochic acids in mice. *J Pharm Pharmacol* 56: 221–229, 2004

53. van Kuppevelt TH, Dennissen MA, van Venrooij WJ, Hoet RM, Veerkamp JH: Generation and application of type-specific anti-heparan sulfate antibodies using phage display technology. Further evidence for heparan sulfate heterogeneity in the kidney. *J Biol Chem* 273: 12960–12966, 1998

54. Challa AA, Vukmirovic M, Blackmon J, Stefanovic B: Withaferin-A reduces type I collagen expression in vitro and inhibits development of myocardial fibrosis in vivo. *PLoS ONE* 7: e42989, 2012

55. van Waarde MA, van Assen AJ, Kampinga HH, Konings AW, Vujaskovic Z: Quantification of transforming growth factor-beta in biological material using cells transfected with a plasminogen activator inhibitor-1 promoter-luciferase construct. *Anal Biochem* 247: 45–51, 1997

56. Livak KJ, Schmittgen TD: Analysis of relative gene expression data using real-time quantitative PCR and the 2(-$\Delta\Delta$ C(T)) Method. *Methods* 25: 402–408, 2001

Q:10